Marine Pollution Bulletin 122 (2017) 456–463

Contents lists available at ScienceDirect

Marine Pollution Bulletin

journal homepage: www.elsevier.com/locate/marpolbul

Baseline

Determination of sedimentation, diffusion, and mixing rates in coastal sediments of the eastern Red Sea via natural and anthropogenic fallout radionuclides

Bandar A. Al-Mur[a,b], Andrew N. Quicksall[b,*], James M. Kaste[c]

[a] Department of Environmental Sciences, King Abdul-Aziz University, Jeddah 21589, Saudi Arabia
[b] Civil and Environmental Engineering, Southern Methodist University, Dallas, TX 75275, USA
[c] Geology Department, College of William & Mary, Williamsburg, VA 23188, USA

ARTICLE INFO

Keywords:
Red Sea
Jeddah
Radionuclide
Sedimentation rate
Chemical diffusion
Particle mixing

ABSTRACT

The Red Sea is a unique ecosystem with high biodiversity in one of the warmest regions of the world. In the last five decades, Red Sea coastal development has rapidly increased. Sediments from continental margins are delivered to depths by advection and diffusion-like processes which are difficult to quantify yet provide invaluable data to researchers. Beryllium-7, lead-210 and ceseium-137 were analyzed from sediment cores from the near-coast Red Sea near Jeddah, Saudi Arabia. The results of this work are the first estimates of diffusion, mixing, and sedimentation rates of the Red Sea coastal sediments. Maximum chemical diffusion and particle mixing rates range from 69.1 to 380 $cm^{-2}\,y^{-1}$ and 2.54 to 6.80 $cm^{-2}\,y^{-1}$, respectively. Sedimentation rate is constrained to approximately 0.6 cm/yr via multiple methods. These data provide baselines for tracking changes in various environmental problems including erosion, marine benthic ecosystem silting, and particle-bound contaminant delivery to the seafloor.

The Red Sea represents a complex marine ecosystem with unique biological diversity and an important shipping lane linking the world's major oceans (Ghandour et al., 2014). The Red Sea comprises the main route from Europe to India and Eastern Asia and is linked with the Indian Ocean at the southeastern end (Chung et al., 1982). The coastline of the Kingdom of Saudi Arabia is about 1840 km in length, accounting for 79% of the eastern seaboard of the Red Sea (Pan et al., 2011). Saudi Arabia has undergone a rapid transformation from an under-developed state, with severe constraints, to a modern industrial country (Badr et al., 2009; Al-Mur et al., 2017). The impact of anthropogenic activities on the sediments of the Red Sea has increased and become a major concern (Badr et al., 2009; Pan et al., 2011; Ghandour et al., 2014, Al-Mur et al., 2017). Despite its ecological importance, high biodiversity and endemism, the Red Sea region has been the subject of relatively few research studies (Berumen et al., 2013). There is a lack of information about the concentrations of natural and anthropogenic radionuclides from Saudi Arabian coastal regions of the Red Sea. There are no quantitative data in the current body of literature showing the chemical diffusion, mixing, or sedimentation rates from the eastern side of the Red Sea. Thus collection of these data is vital to understanding many processes including the behavior of contaminants. Contaminants are delivered to depths in sedimentary systems by advection (burial) and diffusion processes; however, these processes can be difficult to quantify in complex ecosystems. There is a clear need to identify the sedimentation processes on the Red Sea via natural and anthropogenic radionuclides. Radionuclides are introduced via fallout from the atmosphere into the marine surface water column and bind to suspended particles by physical, chemical, and biological processes (Kumar et al., 2013). ^{210}Pb is a natural occurring radionuclide and strongly associates with particles that make it a useful tracer (Conrad et al., 2007) and has been the most widely used radionuclide for determining both mixing and sedimentation rates (Cochran, 1985). The ^{210}Pb half-life of 22.3 years makes it a powerful tool in relating sedimentation processes during the last 100 years or more in the marine environment (Zuo et al., 1991). ^{210}Pb is a member of urainum-238 decay series and is identified in sediment samples from supported and unsupported sources. Supported ^{210}Pb is a radioactive decay product of radium-226 (^{226}Ra) with constant activity along a vertical profile of core sediment. However, the unsupported, or excess, ^{210}Pb ($^{210}Pb_{ex}$) is a radioactive decay product from radon-222 (^{222}Rn) gas escaping through the soil pore space to the atmosphere. The ^{222}Rn then decays to ^{210}Pb and attaches to aerosol particles and is delivered to marine surface water via precipitation. The $^{210}Pb_{ex}$ is quickly removed from the water column; it binds to

* Corresponding author.
E-mail address: aquicksall@smu.edu (A.N. Quicksall).

http://dx.doi.org/10.1016/j.marpolbul.2017.05.054
Received 25 April 2017; Received in revised form 18 May 2017; Accepted 22 May 2017
Available online 27 May 2017
0025-326X/ © 2017 Published by Elsevier Ltd.

sediments due to its strong affinity for particulate matter (Martín et al., 2014) thereby increasing the initial ^{210}Pb content of the sediment (De Vleeschouwer et al., 2010). The $^{210}Pb_{ex}$ activity decreases with its age according with radioactivity decay law. This law can be used as a tool to estimate sedimentation and diffusion rates in marine environments (Szmytkiewicz and Zalewska, 2014).

The isotope ^{210}Pb is a tracer for sediments deposited during a time of approximately 150 years ago through present time due to its half-life ($T_{1/2}$ = 22 years). This period of time is disproportionately important due to changes in the environment from human impact such as urbanization and industrialization (Ruiz-Fernández et al., 2009). However, the natural occurring radionuclide ^{210}Pb chronology is often corroborated by the anthropogenic radionuclide ^{137}Cs ($T_{1/2}$ = 30.1 years) measurement (Ruiz-Fernández et al., 2009). The radionuclide ^{137}Cs is commonly used as an independent tracer to confirm the ^{210}Pb age dating method (Dai et al., 2007). In fact, ^{210}Pb and ^{137}Cs, both sourced from the atmosphere, are used as standard tools to determine sedimentation rates over the last 150 years in sediment environments (Conrad et al., 2007). ^{137}Cs is present in the environment mostly due to global scale fallout from the atmospheric testing of nuclear weapons. The initial testing occurred in the early 1950s and peaked in 1963. The use of ^{137}Cs, therefore, relies on identifying its peak atmospheric deposition that took place in 1963 (Ruiz-Fernández et al., 2009). Generally, both ^{210}Pb and ^{137}Cs provide two independent measurements of estimating the same burial processes happening within a specified sediment profile (Ruiz-Fernández et al., 2009). Typically, ^{210}Pb activities assign an age to each layer of sediment from the surface down, and the presence of ^{137}Cs in the layers assigned to 1955–1966 is used as an independent check on the ^{210}Pb chronology.

Beryllium 7 (^{7}Be) is a naturally occurring radionuclide and is produced in the earth's atmosphere from spallation of gas molecules (Olsen et al., 1981). It has a strong affinity by adsorption for particulate matter after being delivered to the air-water interface (Kaste et al., 2011). ^{7}Be, a short-lived radioactive nuclide ($T_{1/2}$ = 53 day), is a powerful tool for examination of environmental processes (Olsen et al., 1985). It can provide information on diffusion processes of the ocean layer, but it a poor tracer of sedimentation rates in natural environments due to its short half-life of 53 days (Bloom and Crecelius, 1983). Mixing by physical or biological activities alter the rate of dissolution of minerals and can speed up reactions (Henderson et al., 1999). The typical advection-diffusion model includes the effect of particle mixing, sediment accumulation, and radioactive decay (Cochran, 1985). A significant consideration in any study is to determine rate of particle mixing in time scale and use of tracers with different half-life to characterize mixing in a signal core to check on the reliability of mixing rate (DeMaster and Cochran, 1982). The mixing rate can be determined via radionuclides, though difficult, as diffusional mixing competes with decay (Henderson et al., 1999). Mixing of sediments (physical and biological processes) often complicates the use of radionuclide activity in shallow estuarine environments (Conrad et al., 2007). Determining the sedimentation rate is usually a complicated task because both advection (burial) and diffusion-like processes control the distribution of radionuclides with depth in the core (Szmytkiewicz and Zalewska, 2014). Currently there are no published radionuclide measurements in coastal sediments of the eastern Red Sea. Furthermore, there are no quantitative data available regarding sedimentation processes in marine sediments in same region. In this paper, we focus on quantifying the chemical diffusion and particle mixing as well as the sedimentation rates for sediments of the Red Sea near Jeddah. These data are critical in establishing a baseline of sediment processes for future work in a rapidly developing area.

Two sediment cores were collected in January 2015 near the coast of Jeddah along the Red Sea for this study. The Prince Naif and the Downtown sites are located in close proximity to central Jeddah city in the Red Sea. Each sampling location was determined using a GPS and located between 39° 6′ 21″ N and 39° 9′ 26″ E, respectively (Fig. 1). The distance of the Prince Naif core site from the shore was approximately 1000 m and in 25 m water depth while the Downtown core site was close to the shore, about 10 m, and in 2 m water depth (Table 1). Sediment cores were collected by scuba divers; using PVC tubes of 50 cm long and 4.5 cm in diameter. The cores were kept in an icebox at 4 °C until delivered to the laboratory for analysis. After core samples were obtained at selected locations across the study area, samples were stored frozen at − 20 °C for 24 h.

Radionuclides were measured in sediment samples by ultra-low background gamma counting on Canberra Broad Energy 5030 high purity Intrinsic Ge detectors housed in the Geology Department at the College of William & Mary. These detectors were designed with ultra-low background cryostat hardware and remote detector chambers housed in copper-lined 1000 kg + lead shields. Typically, 10–15 oven-dried grams of sediment were packed into 12 mL plastic petri dishes that were sealed in paraffin wax to retain ^{222}Rn. After 3 weeks, ^{210}Pb, ^{226}Ra, ^{7}Be, ^{137}Cs and ^{40}K were determined at 46 keV, 352 keV (via ^{214}Pb), 477 keV, 662 keV and 1461 keV respectively. Detector efficiency at these energies for ^{238}U series radionuclides was determined using certified uranium ore (Canadian Certified Reference Materials Project BL-4a) measured in the identical geometry as the samples, but efficiencies for ^{40}K and ^{137}Cs were determined using a calibrated multinuclear solution containing ^{137}Cs and radionuclides decaying up through 1800 keV (Isotope Products). To keep counting errors below 8%, samples were typically counted for 72–100 h. All ^{210}Pb measurements were corrected for self-attenuation using the point-source method (Cutshall et al., 1983). Typical 2-sigma uncertainties for $^{210}Pb_{ex}$ were 2.5 Bq/kg, which was largely controlled by uncertainty in the supported ^{210}Pb; uncertainties for ^{7}Be and ^{137}Cs are 0.5 and 0.2 Bq/kg, respectively, and are largely controlled by counting statistics (Kaste et al., 2011).

In this study, we calculated the maximum chemical diffusion and sediment mixing rates by using the advection-diffusion model. The overall equation describing the excess ^{210}Pb sediment profile controlled by the following equation (Roberts et al., 1997):

$$\frac{dA}{dt} = D_B\frac{d^2A}{dx^2} - S\frac{dA}{dx} - \lambda A \quad (1)$$

where D_B is the diffusion-like particle mixing rate ($cm^{-2}\,yr^{-1}$); S is the sedimentation rate (cm/yr); A is the activity of excess ^{210}Pb (Bq/kg); x is the depth (cm); and λ is ^{210}Pb radioactive decay constant ($0.03114\ y^{-1}$). If the sediment rate term is considered negligible, this equation is reduced to:

$$\frac{dA}{dt} = D_B\frac{d^2A}{dx^2} - \lambda A \quad (2)$$

Then, the solution under the conditions of $A = A_0$ when $x = 0$ and $A \to 0$ as $x \to \infty$ is:

$$A = A_0 \exp\left[-\left(,\frac{\lambda}{D_B}\right)^{\frac{1}{2}}x\right] \quad (3)$$

Two models of ^{210}Pb activities versus the vertical profiles were applied to determine the rate of sedimentation in the sediment of the Red Sea. The first model is known as Constant Initial Concentration (CIC) model assumes that the system is in a steady state and a constant flux of ^{210}Pb from the atmosphere and rate of sedimentation deposition is constant as well (Szmytkiewicz and Zalewska, 2014). The profiles of excess ^{210}Pb activity were modeled using the constant initial activity and constant accumulation rate assumption as the following equation (Appleby and Oldfield, 1992):

$$C_m = C_{(0)}e^{-\lambda m/r} \quad (4)$$

where $C_{(m)}$ is $^{210}Pb_{ex}$ activity at cumulative dry mass depth (Bq/kg); $C_{(0)}$ is the activity of excess ^{210}Pb at the surface layer of the sediment core (Bq/kg); λ is the ^{210}Pb radioactive decay constant ($0.03114\ y^{-1}$);

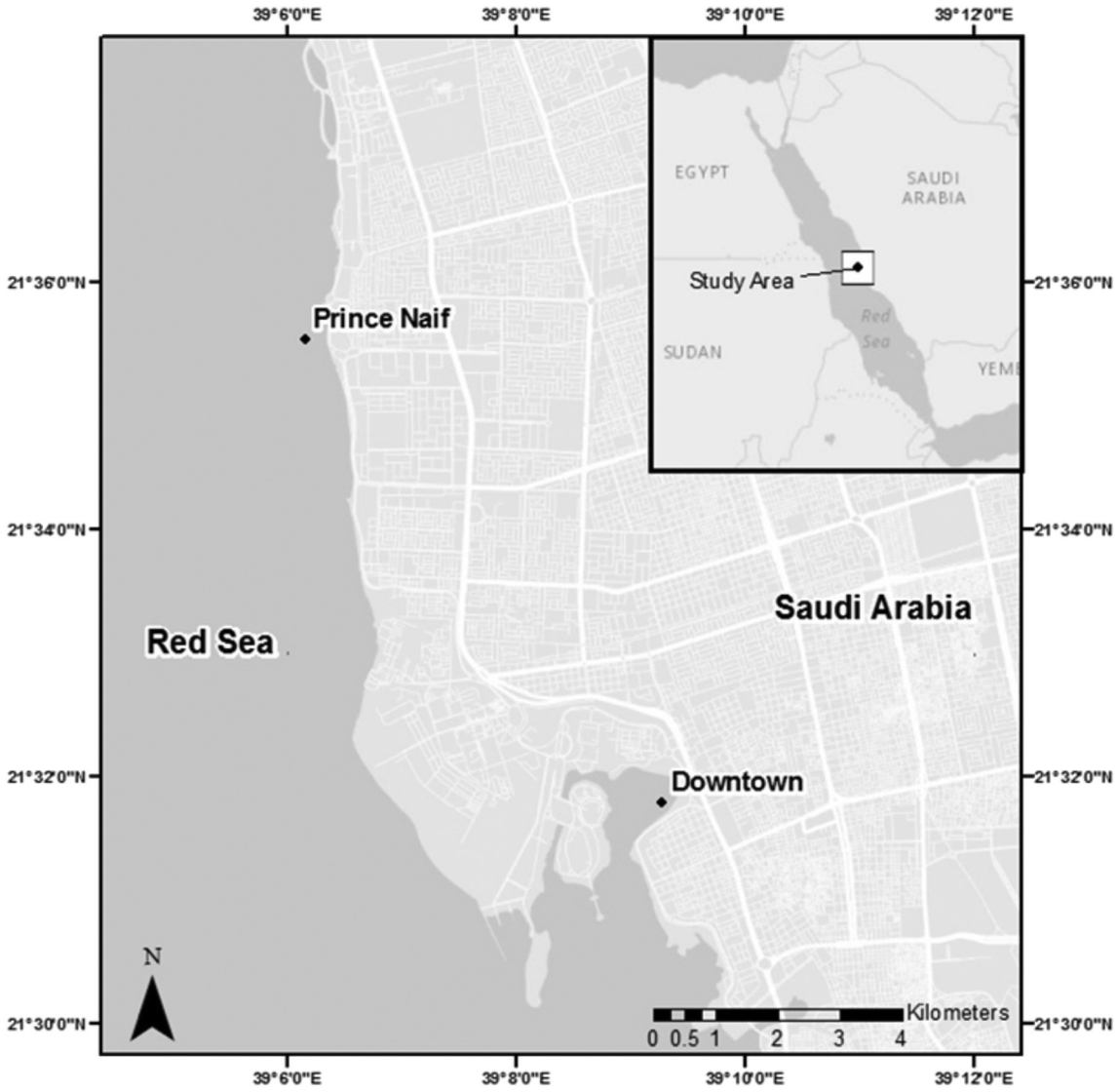

Fig. 1. Location map of the Prince Naif and the Downtown sites in the Red Sea.

Table 1
Locations of sampling sites of collecting cores samples.

Sampling site	Location		Distance from shore (m)	Depth (m)	Core length (cm)
	Latitude	Longitude			
Prince Naif	21° 35′ 33″	39° 6′ 21″	1000	25	50
Downtown	21° 31′ 45″	39° 9′ 26″	10	2	50

m is the cumulative dry mass (g cm^{-2}); and r is the sedimentation accumulation rate (g $cm^{-2}\,yr^{-1}$). As a result, sedimentation rate was determined from the slope of the line regression of the $^{210}Pb_{ex}$ profile and the depth layer. The second model, known as Constant Rate of ^{210}Pb Supply model (CRS), was established by Krishnaswamy et al. (1971) and developed by Appleby and Oldfield (1992). CRS assumes that there is constant fallout of ^{210}Pb to the marine water from the atmosphere in time regardless of variation in the mass accumulation rate. In the environmental changes that occurred, the rate of sediment accumulation or erosion may be very significant during the past 150 years and the ^{210}Pb profile may be expected to be non-linear (Lubis, 2006). The CRS model is used to determine the age of sediment at a given depth from the ^{210}Pb profile according to the following equation (Appleby and Oldfield, 1992):

$$t = \frac{1}{\lambda} \ln \frac{C_{(0)}}{C_m} \quad (5)$$

where t is age (year); λ is the ^{210}Pb radioactive decay constant (ln(2)/$T_{1/2}$); $C_{(0)}$ is total inventory of $^{210}Pb_{ex}$ in the sediment column (Bq/kg); and $C_{(m)}$ is the cumulative inventory of excess ^{210}Pb in the sediment column beneath depth m (Bq/kg). However, sedimentation rate via ^{137}Cs data can be calculated in the sediment as follows (Ruiz-Fernández et al., 2009):

$$S = \frac{d}{(t_{(0)} - 1963)} \quad (6)$$

where S is an average sedimentation rate (cm/yr), $t_{(0)}$ is collected sampling year, d is the depth (cm) of the ^{137}Cs peak from the sediment profile.

The concentration results of radionuclide analyses in sediment layers using gamma spectrometry are shown in Table 2 for the Prince Naif site and in Table 3 for the Downtown site. In this study, ^{7}Be data were presented in the top layers in both sediment cores and decreased with depth (Tables 2 and 3). The measured ^{7}Be concentrations in the sediment-water interface were 15.6 Bq/kg at the Prince Naif site and 78.8 Bq/kg at the Downtown site. The depth of diffusion determined by ^{7}Be ranged from 7 to 9 cm in sediment profile cores of the Red Sea. The activity concentrations of total ^{210}Pb were found to be highest in the

Table 2
Radionuclide activity (Bq/kg) results in sediment at the Prince Naif location.

Depth (cm)	Total ^{210}Pb	^{137}Cs	^{7}Be
0–2	22.2		15.63
2–4	19.8		10.15
4–6	19.2	0.36	5.74
6–8	12.8		3.31
8–10	11.8	0.42	
10–12	12.8		
12–14	12.1	0.20	
14–16	12.7		
16–18	14.2		
20–22	13.6		
22–24	13.5		
28–30	13.8		
32–34	12.2	0.26	
36–38	8.4		
38–40	10.4		

Table 3
Radionuclide activity (Bq/kg) results in sediment at the Downtown location.

Depth (cm)	Total ^{210}Pb	^{137}Cs	^{7}Be
0–6	60.4	1.34	78.79
6–12	47.1	1.39	40.28
12–16	48.4	0.46	
16–20	47.6	0.96	
20–24	34.6	0.68	
24–28	27.7	0.65	
28–32			
32–36	28.5	0.60	
36–38			
38–40			
40–42			
42–46	15.5	0.29	
46–48	19.1	0.45	

upper segments of the sediment cores compared to lower depth subsamples of both sampling sites (Fig. 2). The results show that the supported ^{210}Pb was 13.3 Bq/kg at the Prince Naif site and 17.3 Bq/kg at the Downtown site.

Supported ^{210}Pb was calculated differently between the two cores. The $^{210}Pb_{ex}$ activities for the Downtown core site were determined by subtracted the average of the bottom two depth intervals from the total ^{210}Pb activity. These two points are interpreted to be the only section of the core where $^{210}Pb_{ex}$ is exhausted and therefore represents solely supported ^{210}Pb. However, for the Prince Naif site, the constant activity of ^{210}Pb in the middle of the core was subtracting from the total ^{210}Pb to calculate the $^{210}Pb_{ex}$. The $^{210}Pb_{ex}$ concentrations at the sediment-water interface were 8.92 Bq/kg in the Prince Naif site and 43.1 Bq/kg in the Downtown site. The profiles of ^{137}Cs from both sediment sites are presented in Fig. 6. In the Downtown site, ^{137}Cs activities were detected down core layers to the 46–48 cm interval. However, the activities of ^{137}Cs are only above detection to 32 cm interval in the Prince Naif site.

Two sediment cores from the coastal Red Sea in close proximity to Jeddah were analyzed for radionuclide activities (Fig. 1). ^{7}Be is known to be soluble in marine environments (Bloom and Crecelius, 1983) and this increase in solubility would be exacerbated in a high saline environment such as the Red Sea. In this study, we used ^{7}Be as a tracer of rapid chemical diffusion to track chemical diffusion in marine sediments. However, ^{210}Pb is most likely particle bound and is highly immobile in the Red Sea sediments as indicated by Chung et al. (1982). We, therefore, used ^{210}Pb in this study as a tracer of sediment burial or particle diffusion (mixing). While all processes are likely present this yields effective end members. Maximum chemical diffusion and particle mixing rates were determining by assuming sedimentation rates are zero by using Eq. (2). Significant correlations are obtained between ^{7}Be and $^{210}Pb_{ex}$ activity concentrations and depth as is shown in Figs. 3 and 4. This graphically represents the linear solution to the advection diffusion model when sedimentation is zero. The chemical diffusion rates in the sediment were 69.1 $cm^{-2}\,yr^{-1}$ at the Price Naif site and 380 $cm^{-2}\,yr^{-1}$ at the Downtown site obtained from ^{7}Be data (Fig. 3). However, the results show that the maximum particle mixing rate,

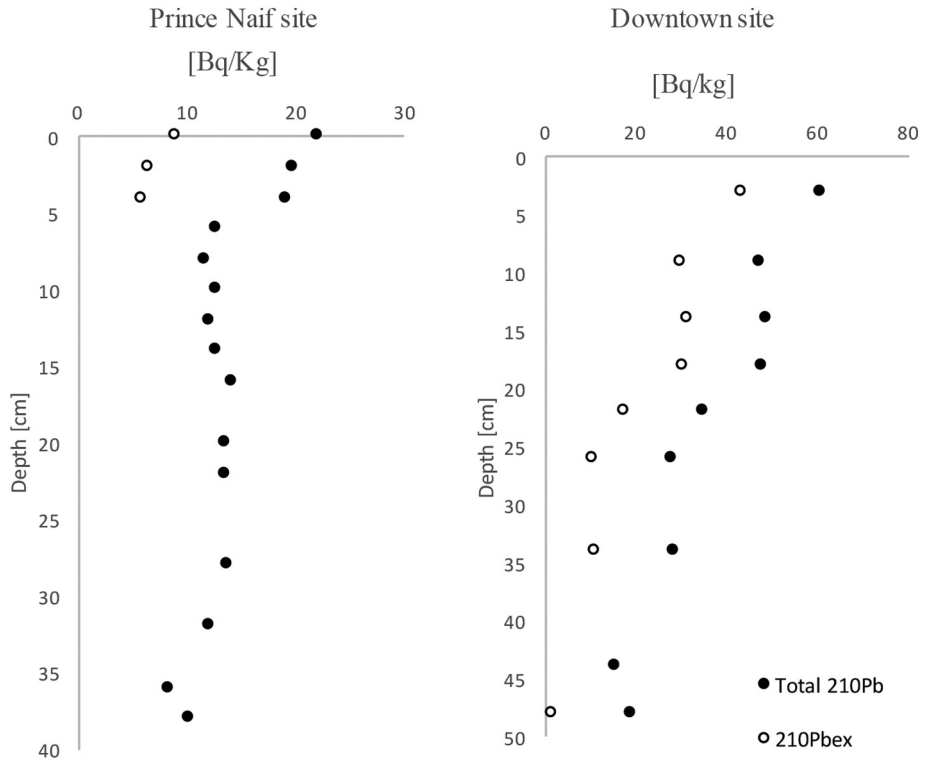

Fig. 2. Total ^{210}Pb and $^{210}Pb_{ex}$ (Bq/kg) at the Prince Naif and the Downtown sites in the Red Sea.

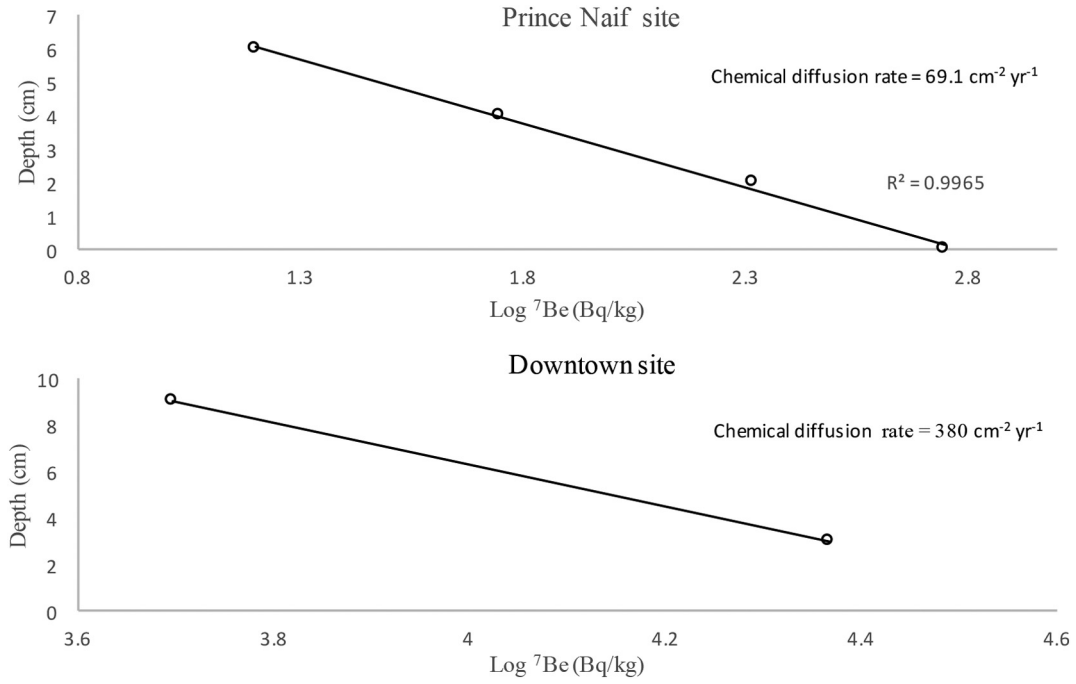

Fig. 3. Maximum chemical diffusion rates calculated driving by ^{7}Be in the Prince Naif and Downtown sites.

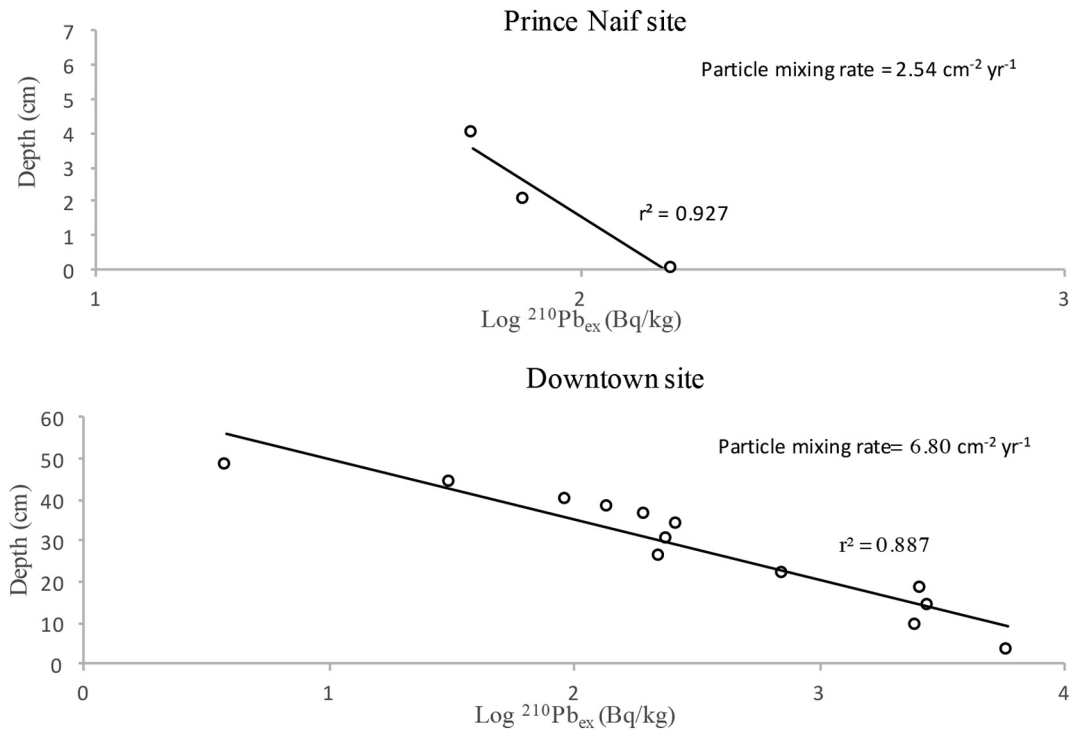

Fig. 4. Maximum particle mixing rates calculated driving by ^{210}Pb in the Prince Naif and Downtown sites.

Table 4
Maximum chemical diffusion and particle mixing rate determined from ^{7}Be and ^{210}Pb profiles.

Sample site	Depth of diffusion	Maximum chemical diffusion ^{7}Be-derived	Maximum particle mixing ^{210}Pb-derived
Prince Naif	7	69.1	2.54
Downtown	9	380	6.80

Depth of diffusion: cm, Chemical diffusion and Mixing rates unit: cm^{2}/y.

derived by ^{210}Pb, was 2.54 $cm^{-2}\,yr^{-1}$ at the Price Naif site and 6.80 cm^{-2} at the Downtown site (Fig. 4). The values calculated for chemical diffusion and particle mixing rate of sediments are summarized in Table 4. The high chemical diffusion and particle mixing at the Downtown site compare to the Prince Naif site indicate that high biological and physical mixing. This is expected given the site's proximity to shore and shallow depth. The biological mixing is due to abundant benthic fauna (Roberts et al., 1997) or a result of infauna activity (Carvalho et al., 2011). Information regarding the benthic fauna near the sampling sites of the Red Sea is limited. The typical natural coastal Saudi Arabia habitat contains mangrove swamps, coral

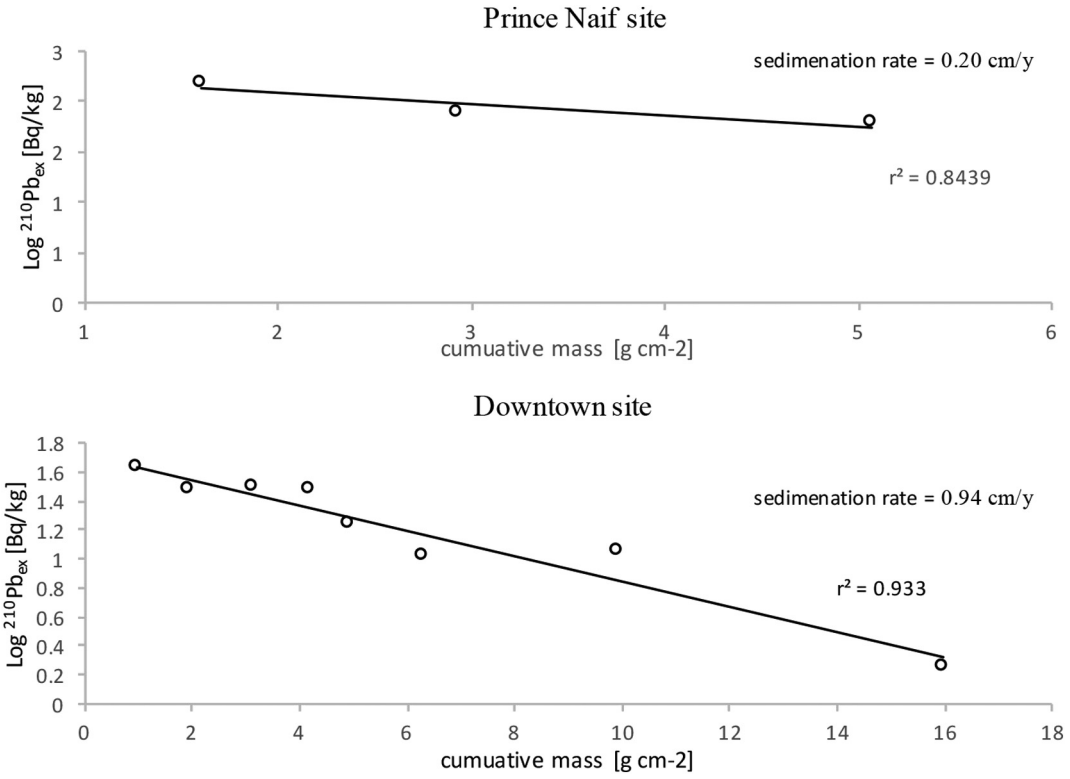

Fig. 5. Logarithmic $^{210}Pb_{ex}$ activity versus cumulative dry mass and calculated maximum sedimentation rate in the two sites via CIC model.

Table 5
Analysis data using CRS model to calculate the age dating and maximum sedimentation rates of sediments at the Prince Naif area.

Depth (cm)	Mass flux (kg/m^2)	Total ^{210}Pb (Bq/kg)	Supported ^{210}Pb (Bq/kg)	$^{210}Pb_{ex}$ (Bq/kg)	Inventory $^{210}Pb_{ex}$ (Bq/m^2)	Inventory $^{210}Pb_{ex}$ (sum) (Bq/m^2)	Estimated year (y)	Date (y)	Maximum Sedimentation rate (cm/y)
0–2	16.00	22.17	13.4	8.77	140.3	140.3	16.5	1998	0.12
2–4	13.31	19.83		6.42	85.5	225.8	33.5	1982	0.12
4–6	21.31	19.17		5.77	122.9	348.7	38.5	1977	0.16
								Average	0.13

Table 6
Analysis data using CRS model to calculate the age dating and maximum sedimentation rates of sediments at the Downtown area.

Depth (cm)	Mass flux (kg/m^2)	Total ^{210}Pb (Bq/kg)	Supported ^{210}Pb (Bq/kg)	Excess ^{210}Pb (Bq/kg)	Inventory Excess ^{210}Pb (Bq/m^2)	Inventory Excess ^{210}Pb (sum) (Bq/m^2)	Estimated year (y)	Date (y)	Maximum Sedimentation rate (cm/y)
0–6	9.87	60.35	17.29	43.06	424.94	424.94	6.19	2009	0.97
6–12	9.47	47.12		29.83	282.41	707.35	11.08	2004	1.08
12–16	12.05	48.43		31.14	375.09	1082.44	18.99	1996	0.84
16–20	10.34	47.62		30.33	313.71	1396.15	27.55	1987	0.73
20–24	7.63	34.58		17.29	131.93	1528.08	31.96	1983	0.75
24–28	13.77	27.74		10.45	143.81	1671.90	37.57	1977	0.75
28–32	23.93	28.11		10.82	258.97	1930.87	51.12	1964	0.63
32–36	12.24	28.49		11.19	137.06	2067.93	61.58	1953	0.58
36–38	15.43	27.14		9.85	151.95	2219.89	79.43	1936	0.48
38–40	5.83	25.80		8.50	49.60	2269.49	88.35	1927	0.45
40–42	8.48	24.45		7.16	60.72	2330.20	104.35	1911	0.40
42–46	14.65	15.52		4.47	65.46	2395.66	142.59	1872	0.32
								Average	0.67

reefs, and seagrass beds (Badr et al., 2009). Shrimp communities live in these sampling sites and the most common species is *Penaeus semisulcatus* (Hariri et al., 2000). The richness of organic matter at the Downtown site appears to control benthic fauna activity and more likely to control the sediment mixing rates in the sediments in sediments of the Red Sea close to Jeddah. This suggestion is similar to the Carvalho et al. (2011) study in sediment accumulation and bioturbation rates in the Northeast Atlantic (Carvalho et al., 2011). They suggested the abundance of organic matter in the deposition flux seems to control fauna activity and biomass and it may play an indirect role in controlling sediment mixing and contaminant mixing rates in the seafloor sediment (Carvalho et al., 2011). In this study, the range of particle mixing rates (2.54 to 6.80 $cm^{-2}\,yr^{-1}$) were within the same order of magnitude reported by Carvalho et al. (2011) paper between 3.1 and 38 $cm^{-2}\,yr^{-1}$ in the coastal environment. Our particle mixing rates were relatively closed to particle mixing rates calculated in deep-

Table 7
Comparison of sedimentation rates as determined by ^{210}Pb and ^{137}Cs.

Sample site	Maximum sedimentation rate via CIC model	Maximum sedimentation rate via CRS model	Maximum sedimentation rate via ^{137}Cs
Prince Naif	0.20	0.13	0.62
Downtown	0.94	0.67	–
Average	0.57	0.40	0.62

Maximum sedimentation rate unit: cm/y.

sea sediments in South Atlantic (DeMaster and Cochran, 1982).

The results of this study show the highest activity of $^{210}Pb_{ex}$ in the uppermost sediment layers and decrease with depth in both cores and useful data to determine the sedimentation rates of the sediments of the Red Sea (Fig. 2). The difference of $^{210}Pb_{ex}$ activities at the sediment-water interface for the two sites suggests that a relatively high spatial or temporal variability of particle size for this region of the Red Sea. Furthermore, radionuclide activities reported by Kumar et al. (2013) to be more concentrated in fine-grained sediment (like in the Downtown site) than in coarse-grained sediments.

The $^{210}Pb_{ex}$ activity (Bq/kg) was plotted on a logarithmic scale against the cumulative dry mass (g/cm^2) to determine the maximum sedimentation rates of sediments via CIC model using Eq. (4). Similar to the approach above for determining mixing and diffusion, here, mixing rates are assumed to be zero in order to calculate the maximum sedimentation rates as a useful end member. The results of the CIC model were a linear ^{210}Pb profile and an R-squared of 0.84 at the Prince Naif site and 0.93 at the Downtown site as shown in Fig. 5. In this study, the best estimate of the maximum sedimentation rate within a CIC model was 0.57 cm/yr. The data analyses for the CRS model for both cores are presented in Tables 5 and 6. Maximum sedimentation rate at the Prince Naif site was 0.13 cm/y, and at the Downtown site was 0.67 cm/yr. Comparison of sedimentation rates via ^{210}Pb profile and ^{137}Cs profile is summarized in Table 7. The average sedimentation rate obtained via the CRS model was 0.4 cm/y. However, in order to verify the results of this study, the estimated average sedimentation rate via the natural occurring radionuclide ^{210}Pb observed is compared with the anthropogenic radionuclide ^{137}Cs activity as an independent dating technique. In this study, ^{137}Cs activities at the Downtown site are presented in all core layers, and it cannot be used as a marker for an age profile of sediment in this site as we are not able to identify the 1963 sediment depth. However, ^{137}Cs is limited to 32 cm in the Prince Naif area and can be used as a marker of age dating of sediment (Fig. 6). The time between sample collection and first peak atmospheric deposition (52 y) yields an average sedimentation rate of 0.62 cm/y compared with 0.57 cm/y calculate from the slope of $^{210}Pb_{ex}$ profile in this site. Therefore, the sedimentation rate between the $^{210}Pb_{ex}$ and ^{137}Cs techniques was close, indicating that both the radioactive isotopes and methods yield comparable results. Our average sedimentation rate value (0.57 cm/y) is much higher than the rate reported by Milliman et al. (1969) (Milliman et al., 1969), which is 0.01 cm/y by the ^{14}C dated technique. Their location is distal from shore (in the middle of the Red Sea); and, therefore, shows little affect from the urbanization that causes increase in sedimentation rate. The average value (0.57 cm/y) of sedimentation rate within this study was in the range reported by Conrad et al. (2007) paper of Elizabeth River in Virginia between 0.5 and 2.0 cm/y and in Jiaozhou Bay in north China between 0.3 and 1.60 cm/y (Dai et al., 2007). Martín et al. (2014) also reported values sediment rates at deep-sea sediment in the Mediterranean Sea from 0.3 to 1.0 cm/y. Therefore, the high sedimentation rates are a common phenomenon in coastal areas especially in recent years due to increasing in delivering of sediments from industry and agriculture (Dai et al., 2007).

Constraints on sedimentation, diffusion, and mixing rates by atmospheric radionuclides were obtained from two sediment cores taken in 2015 from the Red Sea. Chemical, physical, and biological processes vary widely depending on conditions and can be difficult to quantify. In

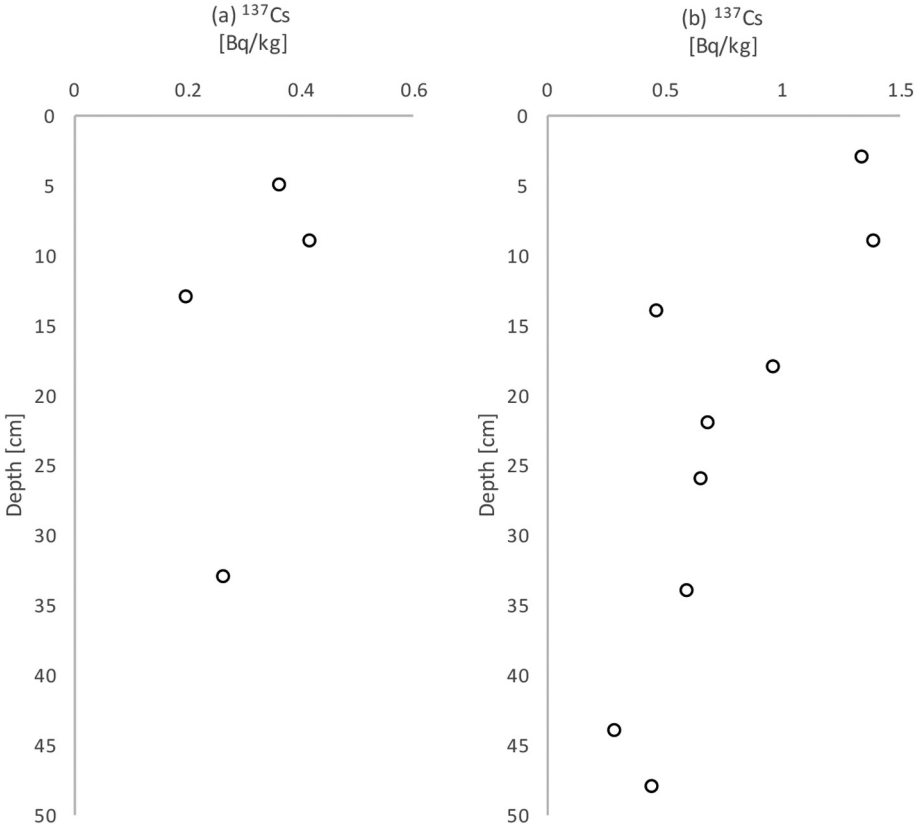

Fig. 6. Profiles of ^{137}Cs at (a) the Prince Naif and (b) the Downtown sites.

this study, the natural occurring radionuclides ^{210}Pb and ^{7}Be as well as the anthropogenic ^{137}Cs were investigated near the coast of Saudi Arabia in Red Sea sediments.

Maximum chemical diffusion and particle mixing rates, from ^{210}Pb and ^{7}Be, show physical mixing and bioturbation to be the likely controlling sedimentation processes close to the shore of the west coast of Saudi Arabia near Jeddah. The profile of ^{7}Be activities showed relatively fast (< 100 days) bed penetration to 7 to 9 cm in some areas. Chemical diffusion rates calculated using ^{7}Be are 69.1 $cm^{-2}\,y^{-1}$ at the Prince Naif site and 380 $cm^{-2}\,y^{-1}$ at the Downtown site. Maximum particle mixing rates calculated by ^{210}Pb data in sediments of the Red Sea ranged from 2.54 to 6.80 $cm^{-2}\,y^{-1}$. Sediment profiles of ^{210}Pb for both Prince Naif and Downtown sites show a decrease in excess activity with depth. Excess ^{210}Pb activity profile decreased in depth to 8 cm in the Prince Naif core site and to 50 cm in the Downtown core site. The average maximum sedimentation rate in two marine sediment cores derived from the ^{210}Pb method is 0.57 cm/y and this value is the first estimate of sedimentation rate for the coastal Red Sea. This robustness of this estimate is augmented by the independent calculation of an estimate from ^{137}Cs; the ^{137}Cs profile peak is 0.62 cm/y.

The research shows the degree to which increased anthropogenic activities from urbanization and economic growth has resulted in high sedimentation rates and sediment mixing close to Jeddah. The outcomes of this work serve as baseline data and can be used for a historical record of environmental contamination in the Saudi Arabian coastal areas on the Red Sea. Many organic and inorganic contaminants are delivered to the marine floor via particle transport and deposition. Tracking the change in sediment delivery, therefore, can yield valuable information in future studies regarding total contaminant delivery. In addition, the results of this study can help researchers to identify areas sensitive to sedimentation. As an example, future studies of change in sedimentation could be linked to impacted marine biodiversity in coastal coral reef ecosystems in the Red Sea.

Acknowledgements

This research was supported by King Abdulaziz University, Jeddah, Saudi Arabia.

References

Al-Mur, B.A., Quicksall, A.N., Al-Ansari, A.M.A., 2017. Spatial and temporal distribution of heavy metals in coastal core sediments from the Red Sea, Saudi Arabia. Oceanologia. http://dx.doi.org/10.1016/j.oceano.2017.03.003.

Appleby, P.G., Oldfield, F., 1992. Applications of lead-210 to sedimentation studies. In uranium-series disequilibrium. Appl. to earth. Mar. Environ. Sci.

Badr, N.B.E., El-Fiky, A.A., Mostafa, A.R., Al-Mur, B.A., 2009. Metal pollution records in core sediments of some Red Sea coastal areas, Kingdom of Saudi Arabia. Environ. Monit. Assess. http://dx.doi.org/10.1007/s10661-008-0452-x.

Berumen, M.L., Hoey, A.S., Bass, W.H., Bouwmeester, J., Catania, D., Cochran, J.E.M., Khalil, M.T., Miyake, S., Mughal, M.R., Spaet, J.L.Y., 2013. The Status of Coral Reef Ecology Research in the Red Sea. pp. 737–748. http://dx.doi.org/10.1007/s00338-013-1055-8.

Bloom, N., Crecelius, E., 1983. Solubility behavior of atmospheric 7Be in the marine environment. Mar. Chem. 12, 323–331.

Carvalho, F.P., Oliveira, J.M., Soares, A.M.M., 2011. Sediment accumulation and bioturbation rates in the deep Northeast Atlantic determined by radiometric techniques. ICES J. Mar. Sci. http://dx.doi.org/10.1093/icesjms/fsr005.

Chung, Y., Finkel, R.C., Kim, K., 1982. 226Ra, 210Pb and 210Po in the Red Sea. Earth Planet. Sci. Lett. 58, 213–224.

Cochran, J.K., 1985. Particle mixing rates in sediments of the eastern equatorial Pacific: evidence from 210Pb, 239,240 Pu and 137Cs distributions at MANOP sites. Geochim. Cosmochim. Acta 49, 1195–1210.

Conrad, C.F., Fugate, D., Daus, J., Chisholm-Brause, C.J., Kuehl, S.a., 2007. Assessment of the historical trace metal contamination of sediments in the Elizabeth River, Virginia. Mar. Pollut. Bull. 54, 385–395. http://dx.doi.org/10.1016/j.marpolbul.2006.11.005.

Cutshall, N.H., Larsen, I.L., Olsen, C., 1983. Direct analysis of 210Pb in sediment samples: self-absorption corrections. Nucl. Inst. Methods Phys. Res. A 206, 309–312.

Dai, J., Song, J., Li, X., Yuan, H., Li, N., Zheng, G., 2007. Environmental changes reflected by sedimentary geochemistry in recent hundred years of Jiaozhou Bay, North China. Environ. Pollut. http://dx.doi.org/10.1016/j.envpol.2006.10.005.

De Vleeschouwer, F., Sikorski, J., Fagel, N., 2010. Development of lead-210 measurement in peat using polonium extraction. In: A Procedural Comparison. 36 (ISSN 1897–1695). http://dx.doi.org/10.2478/v10003-010-0013-5.

DeMaster, D.J., Cochran, J.K., 1982. Particle mixing rates in deep-sea sediments determined from excess 210Pb and 32Si profiles. Earth Planet. Sci. Lett. 61, 257–271.

Ghandour, I.M., Basaham, S., Al-Washmi, A., Masuda, H., 2014. Natural and anthropogenic controls on sediment composition of an arid coastal environment: Sharm Obhur, Red Sea, Saudi Arabia. Environ. Monit. Assess. http://dx.doi.org/10.1007/s10661-013-3467-x.

Hariri, K.I., Nichols, P., Krupp, F., Mishrigi, S., Barrania, A., Ali, A.F., Kedidi, S.M., 2000. Strategic Action Programme for the Red Sea and Gulf of Aden Status of the Living Marine Resources in the Red Sea and Gulf of Aden Region and their Management.

Henderson, G.M., Lindsay, F.N., Slowey, N.C., 1999. Variation in bioturbation with water depth on marine slopes: a study on the little Bahamas Bank. Mar. Geol. 160, 105–118. http://dx.doi.org/10.1016/S0025-3227(99)00018-3.

Kaste, J., Bostick, B., Heimsath, A., Steinnes, E., Friedland, A., 2011. Using atmospheric fallout to date organic horizon layers and quantify metal dynamics during decomposition. Geochim. Cosmochim. Acta 75, 1642–1661.

Krishnaswamy, S., Lal, D., Martin, J.M., Meybeck, M., 1971. Geochronology of lake sediments. Earth Planet. Sci. Lett. 11 (1-5), 407–414.

Kumar, A., Karpe, R., Rout, S., Joshi, V., Singhal, R.K., Ravi, P.M., 2013. Spatial distribution and accumulation of 226Ra, 228Ra, 40K and 137Cs in bottom sediments of Mumbai Harbour Bay. J. Radioanal. Nucl. Chem. 295, 835–839.

Lubis, A.A., 2006. Constant rate of supply (CRS) model for determining the sediment accumulation rates in the coastal area using 210 Pb. J. Coast. Dev. 10, 9–18.

Martín, J., Puig, P., Masqué, P., Palanques, A., Sánchez-Gómez, A., 2014. Impact of bottom trawling on deep-sea sediment properties along the flanks of a submarine canyon. PLoS One 9. http://dx.doi.org/10.1371/journal.pone.0104536.

Milliman, J.D., Ross, D.A., Ku, T.-L., 1969. Precipitation and Lithification of Deep-Sea Carbonates in The Red Sea 1‘‘. 39. pp. 724–736.

Olsen, C.R., Simpson, H.J., Peng, T.H., Bopp, R.F., Trier, R.M., 1981. Sediment mixing and accumulation rate effects on radionuclide depth profiles in Hudson Estuary sediments. J. Geophys. Res. 86 (no. C11), 11020–11028.

Olsen, C.R., Larsen, I.L., Lowry, P.D., Cutshall, N.H., Todd, J.F., Wong, G.T.F., Casey, W.H., 1985. No title. Atmos. Fluxes Marsh-soil Invent. 7Be 210Pb. 90. pp. 10487–10495.

Pan, K., Lee, O.O., Qian, P.Y., Wang, W.X., 2011. Sponges and sediments as monitoring tools of metal contamination in the eastern coast of the Red Sea, Saudi Arabia. Mar. Pollut. Bull. 62 (5), 1140–1146. http://dx.doi.org/10.1016/j.marpolbul. 2011.02.043.

Roberts, K.A., Cochran, J.K., Barnes, C., 1997. 210Pb and 239,340Pu in the Northeast water polynya, Greenland: particle dynamics and sediment mixing rates. J. Mar. Syst. 10, 401–413. http://dx.doi.org/10.1016/S0924-7963(96)00061-9.

Ruiz-Fernández, A.C., Frignani, M., Hillaire-Marcel, C., Ghaleb, B., Arvizu, M.D., Raygoza-Viera, J.R., Páez-Osuna, F., 2009. Trace metals (Cd, Cu, Hg, and Pb) accumulation recorded in the intertidal mudflat sediments of three coastal lagoons in the gulf of California, Mexico. Estuar. Coasts. http://dx.doi.org/10.1007/s12237-009-9150-3.

Szmytkiewicz, A., Zalewska, T., 2014. Sediment deposition and accumulation rates determined by sediment trap and 210Pb isotope methods in the outer puck bay (Baltic Sea). Oceanologia. http://dx.doi.org/10.5697/oc.56-1.085.

Zuo, Z., Eisma, D., Berger, G.W., 1991. Determination of sediment accumulation and mixing rates in the Gulf of Lions, Mediterranean Sea. Oceanol. Acta 14, 253–262.